colorants

MDPI

Article

3′-Nitro- and 3′-Aminofluoresceins: Appearance of Previously Missing Dyes

Sergey V. Shekhovtsov [1], Iryna V. Omelchenko [2], Svitlana V. Shishkina [2], Andrey O. Doroshenko [3], Kateryna O. Vus [4], Hanna S. Vlasenko [2] and Nikolay O. Mchedlov-Petrossyan [1,*]

[1] Department of Physical Chemistry, V. N. Karazin Kharkiv National University, 61022 Kharkiv, Ukraine; shekhovtsov@karazin.ua
[2] Institute for Single Crystals, National Academy of Sciences of Ukraine, 61001 Kharkiv, Ukraine; irina@xray.isc.kharkov.com (I.V.O.); sveta12.20@gmail.com (S.V.S.); annavlasenko@gmail.com (H.S.V.)
[3] Department of Organic Chemistry, V. N. Karazin Kharkiv National University, 61022 Kharkiv, Ukraine; andrey.o.doroshenko@karazin.ua
[4] Department of Medical Physics and Biomedical Nanotechnologies, V. N. Karazin Kharkiv National University, 61022 Kharkiv, Ukraine; kateryna.vus@karazin.ua
* Correspondence: mchedlov@karazin.ua

Abstract: Contrary to the 4′- and 5′-nitro- and aminofluoresceins, the corresponding 3′-derivatives are practically unexplored. In this paper, we describe the synthesis and spectral properties of 3′-nitrofluorescein and 3′-aminofluorescein, as well as their methyl esters. Among other methods, X-ray analysis, ^{13}C NMR spectroscopy, and ESI mass spectrometry made it possible to establish the molecular structure of the target compounds as well as intermediates and by-products. Some unexpected products, though in small amounts, were revealed within the course of study. Whereas the fluorescence of the double-charged R^{2-} ion of 3′-nitrofluorescein in both aqueous and organic solvents is weak, the R^{2-} anion of 3′-aminofluorescein in a non-hydrogen bonding donor solvent, but not in water, exhibits intensive fluorescence, analogous to the case of 4′- and 5′-aminofluoresceins. Interestingly, the λ_{max} values in water of the R^{2-} ions bearing an NO_2 group in the 3′- and 6′-positions are 7 to 10 nm higher than those of the 4′- and 5′-nitro derivatives. The difference was also observed in dimethyl sulfoxide. This correlates with the angles between the xanthene and phthalic planes of the dyes. The dye 3′-aminofluorescein could be used as a fluorescent indicator sensitive to hydrogen bonding ability of the solvent. It could also serve as a platform for synthesizing fluorescent molecular probes for biochemical research, analogous to the very popular application of 4′- and 5′-amino derivatives.

Keywords: 3′-nitrofluorescein; 3′-aminofluorescein; synthesis; NMR spectroscopy; X-ray analysis; visible absorption spectra; fluorescence

Citation: Shekhovtsov, S.V.; Omelchenko, I.V.; Shishkina, S.V.; Doroshenko, A.O.; Vus, K.O.; Vlasenko, H.S.; Mchedlov-Petrossyan, N.O. 3′-Nitro- and 3′-Aminofluoresceins: Appearance of Previously Missing Dyes. *Colorants* **2023**, *2*, 500–518. https://doi.org/10.3390/colorants2030024

Academic Editor: Julien Massue

Received: 4 May 2023
Revised: 18 July 2023
Accepted: 21 July 2023
Published: 30 July 2023

1. Introduction

Aminofluoresceins bearing the NH_2 group in either the 4′ or 5′ positions (Figure 1) are widely used as platforms for creating different molecular probes for biochemical and biomedical research [1,2], both for diagnostics [3,4] and photodynamic therapy [3–5]. Normally, they are prepared by reduction of the corresponding nitro derivatives. The latter are obtained by condensation of 4-nitrophthalic acid with resorcinol and separating the 4′- and 5′-nitro isomers [1,2,6]. However, to the best of our knowledge, there is no information on 3′-aminofluorescein in the literature. Moreover, data about the 3′-nitrofluorescein are scarce and conflicting [7–12]. We decided to fill this gap and performed the corresponding synthesis.

As early as 1897, Reverdin [7] reported the preparation of 3′-nitrofluorescein from 3-nitrophthalic acid and resorcinol; the melting point of 215 °C of this product was not

confirmed by our data (see below). Bogert and Wright [8] repeated this synthesis and obtained a product with the same melting point and a nitrogen content agreeing with the calculated value. In alkaline solution, the substance was yellowish-red with weak but distinct green fluorescence.

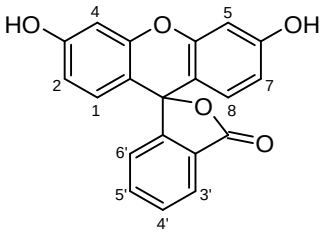

Figure 1. Fluorescein molecule as a lactone tautomer.

Somewhat later, Moir used the same way of synthesis and obtained a product with a salmon color and green fluorescence in alkaline solution [9]. This author was probably not aware of the above-mentioned articles; the absorption maximum reported by him was 495 nm; in the next paper, the author published a value of 500 nm [10]. It should be noted that for fluorescein in aqueous alkaline solutions Moir, reported λ_{max} = 493.5 nm [10], whereas the updated value is 490–490.5 nm [13,14].

Underwood and Wakeman [11] presented a detailed description of their synthesis, which also was based on 3-nitrophthalic acid and resorcinol. Their resorcinol-3-nitrophthalein, i.e., 3′-nitrofluorescein, was obtained with a 17% yield. The solution in sodium hydroxide was brownish-yellow; the determined C, H, and N contents were satisfactory, whereas the melting point was 260 °C. A dilute alkaline solution exhibited a green fluorescence, "but not nearly to the same extent as a solution of fluorescein" [11].

Finally, Hanna and Smith [12] repeated the procedure reported by Underwood and Wakeman and obtained a product with a melting point of 260 °C at a yield of 66% and noted that two isomers, 3′- and 6′-nitrofluoresceins, may be obtained by this method. They also measured the molar absorptivity of the product thus obtained and fluorescein in 95% ethanol. Unfortunately, the pH of the medium was not sufficiently high to obtain the characteristic spectra of the intensively light-absorbing dianionic forms of these dyes. The absorption maxima obtained at $(2.6 - 3.0) \times 10^{-5}$ M were 456 and 458 nm, respectively, and the molar absorptivities at $(3.1 - 4.5) \times 10^{3}$ were rather low; thus, the predominance of the lactonic neutral forms of the dyes could be expected.

In the literature available, we have found no attempts to reduce the above nitro derivative to aminofluorescein.

Therefore, we decided to consider this issue in detail. As a result, both 3′-nitro- and 3′-aminofluoresceins were prepared, identified, and their absorption and fluorescence were characterized. Besides the target compounds, some other reaction by-products were revealed. It turned out that the reaction process is much more complicated than is the case for the synthesis of 4′- and 5′-derivatives. This largely explains the inconsistency of the earlier works [7–12].

It was revealed that the double-charged anion of 3′-aminofluorescein exhibits bright fluorescence in solvents that are not donors of hydrogen bonds, whereas fluorescence in water is poor. It can be assumed that this compound is a potential platform for the synthesis of fluorescent molecular probes for biochemical research, analogous to those mentioned at the very beginning of this article.

2. Results and Discussion

The synthesis was carried out according to the classical method by fusing resorcinol with 3-nitrophthalic acid (Scheme 1). The pathway from **2** to **5** is a standard procedure

[6]. When considering the synthesis scheme developed in our study, it became clear that the authors of the earlier cited works certainly obtained mixtures of different reaction products.

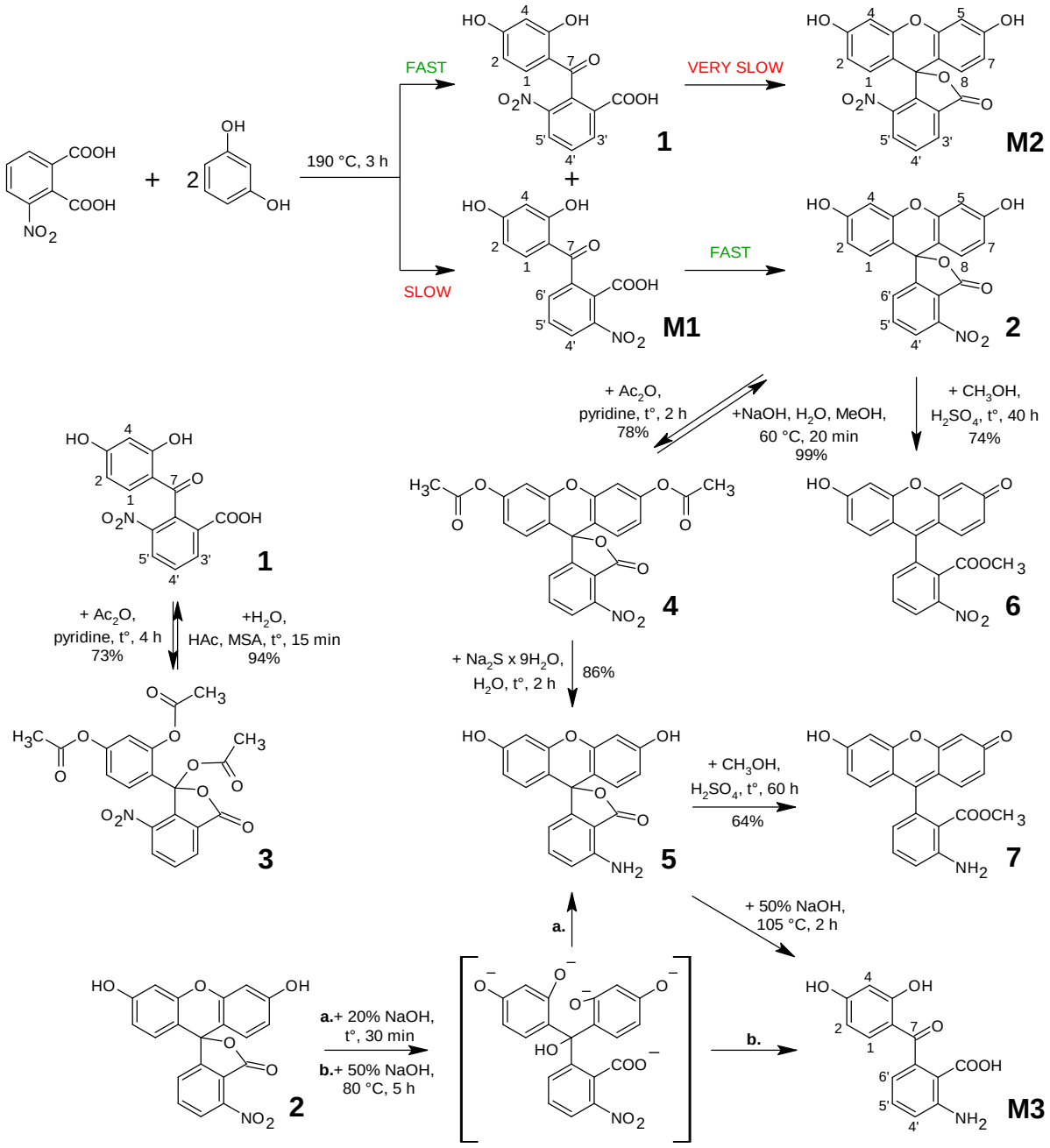

Scheme 1. Synthetic route to 6′-nitrointermediate **1**, 3′-nitrofluorescein **2**, 3′-aminofluorescein **5**, and some of their derivatives. The structure of the assumed reducing agent is shown in square brackets. The letter M denotes the substances that are not isolated in highly pure state, though their identity is proved.

During the reaction, crystals precipitated from the melt, representing a mixture of 3′-nitrofluorescein **2** and 6′-nitrointermediate **1** in a 1:1 molar ratio (NMR). To separate the mixture into **1** and **2**, their different solubility in acetone was used. The yield of product **2** did not exceed 20%. Further purification was carried out through acyl derivatives **3** and **4**, respectively.

Under the synthesis conditions described above, the 6′-nitrofluorescein **M2** isomer is formed in negligible amounts but it can be detected in the NMR spectra.

In a series of experiments, we managed to obtain a small amount of crude 6′-nitrofluorescein by fusing 6′-nitrointermediate **1** with resorcinol in *p*-toluenesulfonic acid.

Reduction of product **4** by sodium sulfide results in 3′-aminofluorescein **5**, according to the described procedure [6]. Esterification of compounds **2** and **5** performed in methanol in the presence of sulfuric acid leads to compounds **6** and **7**, respectively. The structures of the compounds were estimated using the NMR spectra, X-Ray and ESI-MS.

To obtain **M1**, an attempt was made to cleave compound **2** in concentrated NaOH, which is a typical decomposition pathway for xanthenes. Surprisingly, 3′-aminofluorescein **5** was obtained. On further cleavage in still more concentrated alkali, presumably the product **M3** is formed.

Note that the route **2–a.–5** in alkaline solution was revealed in the present study. The final substance was not obtained in pure state; however, its identity as **5** was confirmed using ESI, UV-visible spectra, TLC, and NMR; the content of compound **5** in the above substance was determined by UV-visible spectra (see Section 3.3.4 and the Supplementary Information).

The structure of the reaction products was characterized using ^{13}C NMR and X-ray methods.

The carbon NMR spectra of 3′-nitro and 3′-amino substituted fluoresceins **2** and **5**, respectively, in dimethyl sulfoxide, DMSO, were interpreted by the scheme already used by our research team in our previous papers. The method consists of the calculation of the corresponding spectra in DFT-Giao (b3lyp [15], cc-pvdz [16], GIAO [17], accounting for DMSO polarity in the PCM [18] model using Gaussian 09 software [19]). After that, the correlation of the experimental signal positions in the ^{13}C spectra with the calculated magnetic shielding was built. This scheme helps to identify overlapping signals and check whether the assumed chemical structure of compounds, which can theoretically exist in a mixture of several tautomeric forms, matches the real structures (for example, lactone or zwitter-ion in the cases of fluorescein or rhodamine dyes).

According to our DFT structure simulations, the introduction of a nitro group in the immediate vicinity of the lactone carbonyl C=O induces an increase in steric hindrance, which causes the NO_2 fragment to rotate through an angle of ~38–39°.

As a result, the conjugation of this substituent with the benzene ring is significantly disrupted so its electron density redistribution is mainly controlled by the carbonyl group, while the effect of the nitro group should be much less. In contrast to the 3′-NO_2 group, the amino group in the corresponding position does not experience steric repulsion, it is completely planar, and remains conjugated with the benzofurane moiety. However, the degree of its pyramidalization is significant (the sum of three valence angles at the nitrogen atom of the amino group is ~352.7°), which indicates its substantial sp^3-hybridization character. Despite this, according to the position of the ^{13}C NMR signals, the NH_2 group seems to be the most important factor regulating the electron density redistribution in the benzene ring under discussion. The NH···O distance is about 2.27 Å, which indicates the presence of a weak intramolecular H-bond in the discussed compound. A rough estimate of its energy according to the Espinosa [20] approach within AIM theory [21,22] results in 3.5 kcal/mol only.

The attribution of ^{13}C NMR spectra of nitro- and amino-derivatives of fluorescein possessing substituents in the benzofuranone moiety is presented in Table 1, and the correlations between the calculated magnetic shielding and experimental NMR spectra are shown in Figure 2.

Table 1. ^{13}C NMR spectral data of 3′-nitro- and 3′-aminofluorescein in DMSO-d_6.

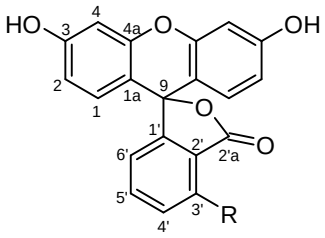

Atom	δ, ppm	Atom	δ, ppm	Atom	δ, ppm
		3′-nitrofluorescein **2**			
1	129.30	9	83.30	1′	159.93
2	108.64			2′	118.06
3	154.37	2′a (C=O)	163.33	3′	145.74
4	102.34			4′	124.71
1a	112.89			5′	136.98
4a	151.95			6′	128.62
		3′-aminofluorescein **5**			
1	128.19	9	81.97	1′	153.59
2	110.51			2′	109.59
3	159.22	2′a (C=O)	169.85	3′	147.58
4	102.08			4′	112.43
1a	113.99			5′	136.47
4a	151.66			6′	107.45

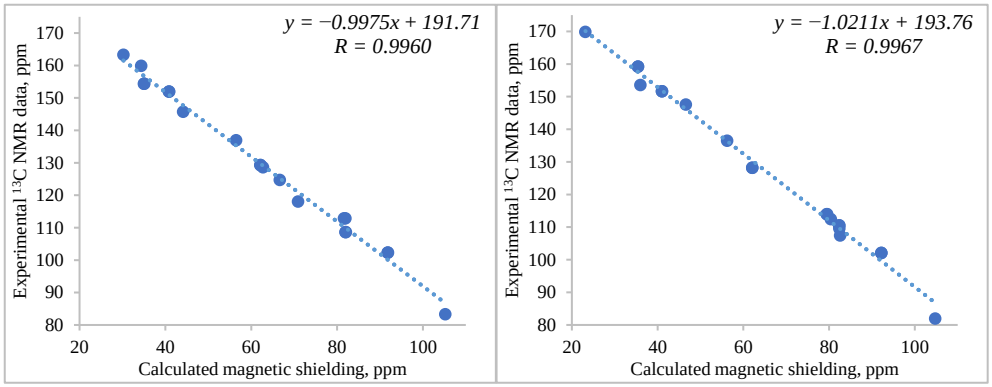

Figure 2. Correlation between the experimental ^{13}C NMR data and calculated magnetic shielding (b3lyp/cc-pvdz) for 3′-nitro- (**left-hand side**) and 3′-aminofluorescein lactone (**right-hand side**).

An analogous approach was used to characterize the acyl derivative of 3′-nitrofluorescein **4** (Table 2, Figure 3) and the 6′-nitrointermediate **3** (Table 3, Figure 3).

Table 2. ^{13}C NMR spectral data of 3′-nitrofluorescein diacetate **4**, in DMSO-*d*$_6$.

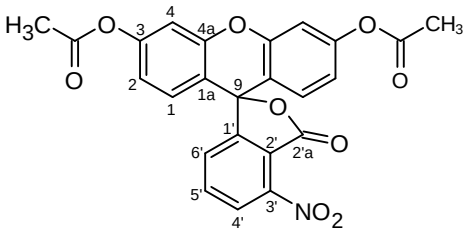

Atom	δ, ppm	Atom	δ, ppm	Atom	δ, ppm
1	128.83	C9	80.49	2′a(C=O)	162.97
2	117.65			1′	154.11
3	152.29	Acetyl groups		2′	118.69
4	110.55	C=O	168.80	3′	145.85
1a	115.03			4′	125.33
4a	150.85	CH_3	20.83	5′	137.44
				6′	129.52

Table 3. ^{13}C NMR spectral data of 6′-nitrointermediate triacetate **3**, in DMSO-*d*$_6$ (the atom numeration scheme presented here is chosen in analogy to that of fluorescein lactone).

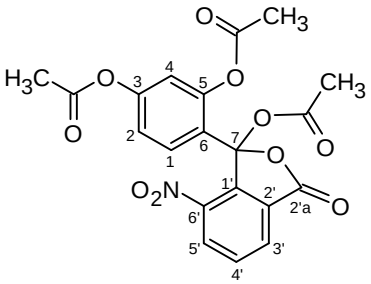

Atom	δ, ppm	Atom	δ, ppm	Acetyl Groups	δ, ppm	
					C=O	CH_3
1′	139.54	1	129.72	at C3	168.28	20.24
2′	130.66	2	116.27	at C5	168.70	20.82
2′a (C=O)	165.62	3	152.06	at C7	167.76	21.26
3′	130.85	4	119.36			
4′	133.86	5	147.60			
5′	131.06	6	123.02			
6′	142.97	7	101.89			

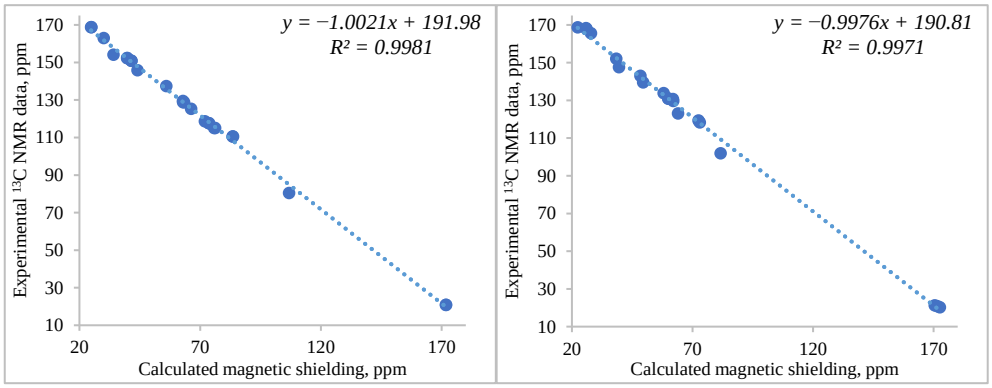

Figure 3. Correlation between the experimental ^{13}C NMR data and calculated magnetic shielding (b3lyp/cc-pvdz) for 3′-nitrofluorescein diacetate **4** (**left-hand side**) and 6′-nitrointermediate triacetate **3** (**right-hand side**).

The structure of the neutral lactone form of compound **4** was confirmed by the X-ray diffraction study (Figure 4). The *spiro* joined xanthene and *iso*-benzofuran fragments are almost orthogonal to each other (the dihedral angle is 87°). All the C–C bonds centered at the *spiro* atom have normal lengths, while the C1–O2 bond (1.464(4) Å) is close to the mean value of the C–O bond in common γ-lactones, 1.464 Å [23]. It should be noted that this bond was longer in fluorescein and its structural analogues studied earlier [24–31]. The pyran ring of the xanthene fragment adopts a boat-like conformation, in which the C3, C2, C8, C9 atoms lie within a plane with an accuracy of 0.007 Å, while the O1 and C1 atoms deviate from this plane by 0.15 Å and 0.23 Å, respectively. Both acetoxy substituents are not coplanar to the aromatic rings (the C12–C11–O8–C23 and C6–C5–O6–C21 torsion angles are 58.8(5)° and 80.0(4)°). The nitro group is rotated with respect to the *iso*-benzofuran bicycle (the O4–N1–C16–C15 torsion angle is 39.7(6)°) to compensate the steric repulsion with the carbonyl C20=O3 group. The last value of the torsion angle is in line with the above DFT estimation for compound **2**; for compound **4** such a calculation gives a value of ~32°.

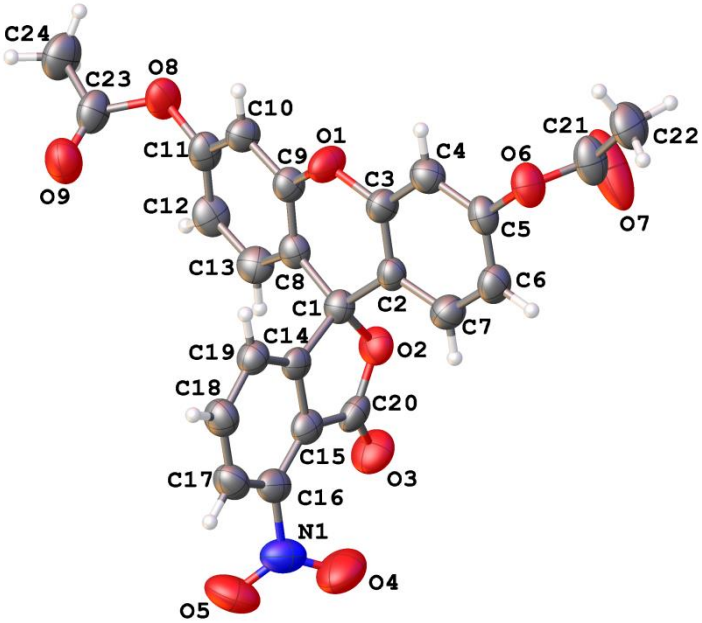

Figure 4. Molecular structure of **4** according to X-ray diffraction study. Atoms are shown as 50% thermal ellipsoids.

The molecular structure of the product **3** was also studied by the X-ray diffraction method (Figure 5). The bicyclic fragment is planar with an accuracy of 0.017 Å. The nitro group is coplanar to the aromatic ring (the O5–N1–C20–C2 torsion angle is −1.6(6)°). Both substituents at the C1 atom are rotated with respect to the bicyclic fragment in such a way that their π-systems are almost orthogonal to the *iso*-benzofuran moiety (the dihedral angles "bicyclic fragment/C8…C13 aromatic ring" and "bicyclic fragment/ester substituent" have the value of 87°). Two acetoxy substituents at the aromatic carbon atoms are rotated with respect to the benzene ring (the C10–C9–O7–C16 and C12–C11–O9–C18 torsion angles are −72.6(5)° and 49.3(5)°).

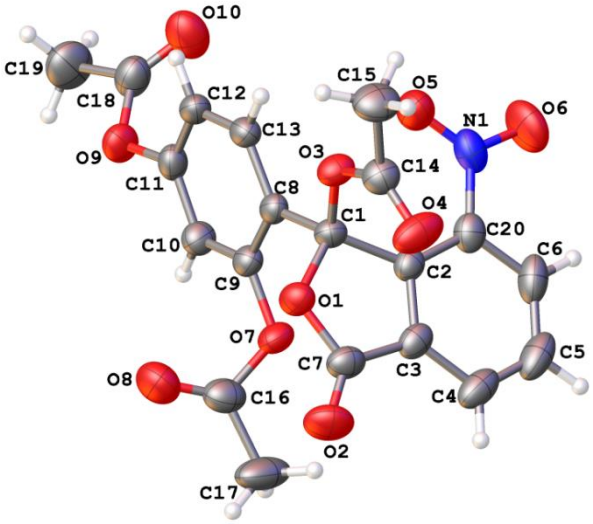

Figure 5. Molecular structure of **3** according to X-ray diffraction study. Atoms are shown as 50% thermal ellipsoids.

The visible absorption and fluorescence spectra of the dianionic forms of the target dyes, R^{2-} are presented in Figure 6 and Table 4. Briefly, 3′-nitrofluorescein exhibits very poor fluorescence both in water and in DMSO, whereas in the case of 3′-aminofluorescein, excellent bright emission is observed in DMSO, acetonitrile, and acetone. The addition of even small amounts of water quenches the fluorescence. These observations completely match those made for 4′-nitrofluorescein and 4′- and 5′-aminofluoresceins in water and non-aqueous solvents [32,33].

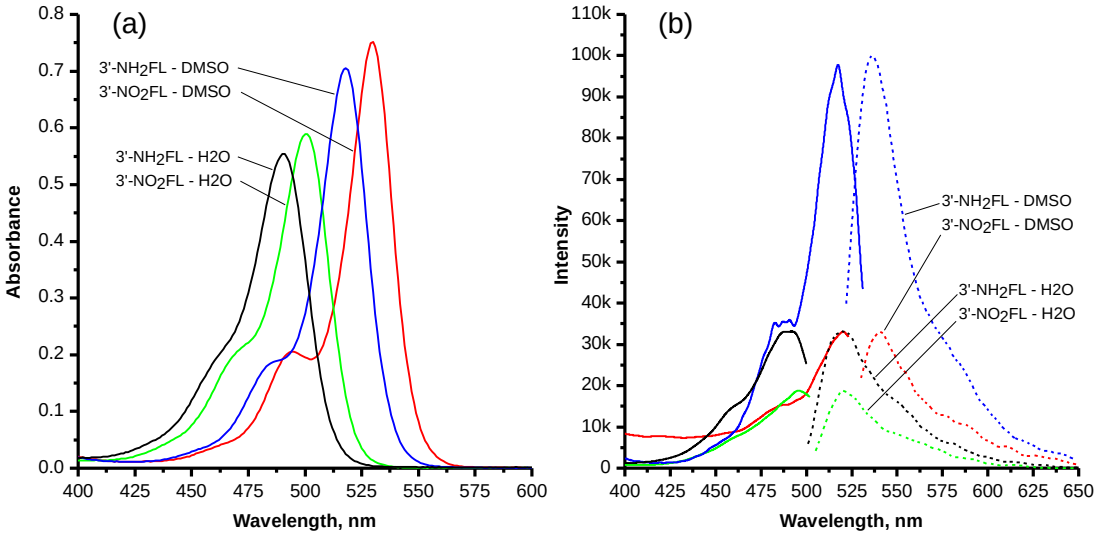

Figure 6. Visible absorption spectra (**a**), and fluorescence excitation (solid line) and emission (dotted line) spectra (**b**) of 3′-nitrofluorescein in water (green) and in DMSO (red), and of 3′-aminofluorescein in water (black) and in DMSO (blue). The aqueous solutions contained 0.16% DMSO by volume and 0.09 M NaOH; the solutions in DMSO contained 0.05 M diazabicyclo [5.4.0]undec-7-ene (DBU). Dyes concentration: 6.40×10^{-6} and 3.20×10^{-6} M for absorption and fluorescence, respectively. The excitation and emission slits for the 3′-aminofluorescein in DMSO system were set to 2.5 nm and in other cases to 10 nm.

Nitro groups can quench the emission of NO_2-substituted fluorescein by several photophysical mechanisms. The most important among them is the acceleration of in-

tersystem crossing (ISC) with population of triplet states [34], which are non-luminescent in fluid solutions. Another possible quenching mechanism includes charge transfer to the electron withdrawing nitro group, for example, see [32,35]. In the case of the aminoderivative, the hydrogen bonds with water molecules quench the emission, whereas in DMSO and other non-hydrogen bond donor solvents, the COO^- group is poorly solvated, and this favors fluorescence [32].

Therefore, it can be stated that only the aminofluorescein, and only in an organic non-hydrogen donor solvent, exhibits intensive fluorescence, which is analogous to the 4′- and 5′-aminofluoresceins [32, 33]. Now the described dye 3′-aminofluorescein can be used in further syntheses for the same purposes as the 4′- and 5′-analogues.

Table 4. Absorption and emission maxima positions and molar absorptivities of the R^{2-} ions of 3′-nitrofluorescein and 3′-aminofluorescein in water and in DMSO.

Dye	Solvent	Absorption		Emission
		λ_{max}, nm	Molar Absorptivity $\times 10^{-3}$, $M^{-1}cm^{-1}$	λ_{max}, nm
3′-Nitrofluorescein	Water	501	92.18	520
3′-Nitrofluorescein	DMSO	530	117.48	541
3′-Aminofluorescein	Water	490	86.63	520
3′-Aminofluorescein	DMSO	518	110.35	536

Another issue is the influence of the position of the nitro group on the λ_{max} position in the R^{2-} spectra (Table 5).

Table 5. Dependence of the absorption maxima of R^{2-} anions on the position of the nitro group in the phthalic acid residue.

Compound	λ_{max}, nm	
	In Water	In DMSO
Fluorescein	490	521
3′-Nitrofluorescein	501	530
4′-Nitrofluorescein	495	526
5′-Nitrofluorescein	494	528
6′-Nitrofluorescein	504	536

Note: Moir reported the following absorption maxima in water: for 3′-nitrofluorescein, 495 nm [9] and 500 nm [10]; and for 5′-nitrofluorescein in water, 498 nm [10]. As it was mentioned in Section 1, these values are probably somewhat overestimated because for fluorescein, Moir reports a value of 493.5 nm. The samples of the 4′-nitrofluorescein and 5′-nitrofluorescein, used for our measurements, were prepared and identified in a standard way; their characterization and acid–base properties were published recently [36].

To elucidate the role of a nitro group in the benzene ring connected to the central carbon atom C(9) in the xanthene ring of the fluorescein dianion, a series of quantum-chemical calculations was carried out in the DFT scheme using *m06-2x* [37] electron density functional and *cc-pvdz* orbital basis [16] with *Gaussian-09* software [19], covering positions of NO_2-substituents in the side phenyl moiety from 3′ to 6′.

Normally, the carboxylate group of fluorescein dianion favors an orthogonal space orientation of the discussed side benzene ring due to weak non-covalent interactions between the partially positively charged C(9) atom and one of the oxygen atoms of the carboxylate group, which carries a partial negative charge. This interaction cannot be considered as completely electrostatic. Its energy can be roughly estimated basing on calculations of the molecular structure of the target system in the framework of Bader's AIM theory [21,22] using the semiempirical Espinosa approach [20]. Its principal application is wider than the initial elucidation of the H-bond energy. (See discussion in ref.

[38].) Universal solvent effects were accounted for only within the PCM model [18]. Typical plots are shown in Figure 7, and the corresponding numerical data are collected in Table 6.

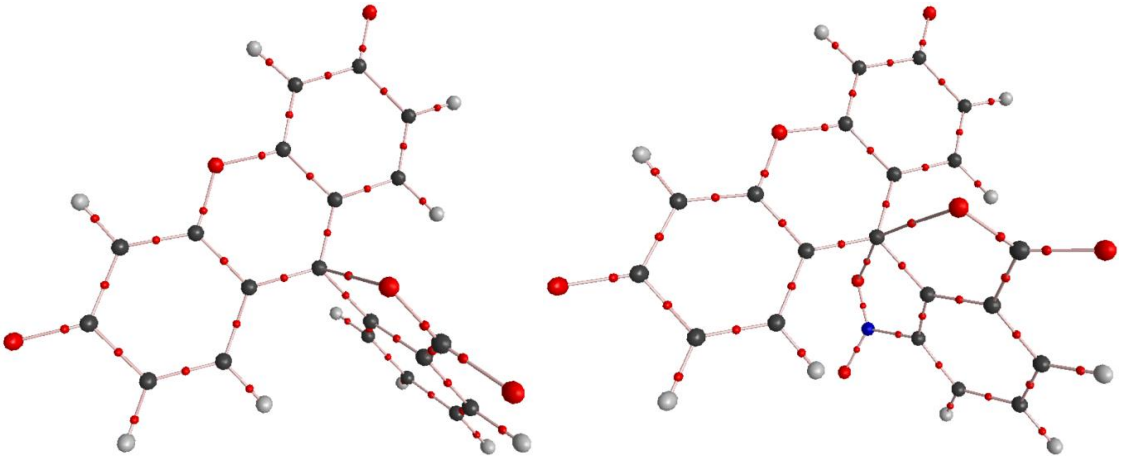

Figure 7. Molecular geometry of fluorescein dianion (**left-hand side**) and its 6′-nitro-derivative (**right-hand side**) calculated in DFT *m06-2x/cc-pvdz* scheme accounting for the solvent (DMSO) effects in the *PCM* model. The color of Atoms is as follows: C – black, H – gray, O – red, and N - blue. Bonds paths and critical points of (3, –1) type according to AIM theory are shown. Weak non-covalent intramolecular interactions NO_2···C(9)···COO^- are clearly observed.

Table 6. Molecular geometry of fluorescein dianion and several its derivatives possessing nitro groups in different positions of the side benzene ring.

Substituent	Angle between Xanthene and Side Benzene Rings Planes, Degrees	C(9)···O Distance, Å, Weak Non-Covalent Intramolecular Interactions Energy, kcal/mol	Electric Charge on C(9) Atom
H	90°	2.67 Å 3.91 kcal/mol	+0.259
3′-NO_2	71°	3.02 Å No bond path found	+0.198
4′-NO_2	90°	2.68 Å 3.82 kcal/mol	+0.257
5′-NO_2	90°	2.68 Å 3.83 kcal/mol	+0.256
6′-NO_2	72°	2.72 Å 3.58 kcal/mol	+0.237

The introduction of a nitro group into position 4′ or 5′ of the side benzene ring does not principally change the geometry of the fluorescein dianion core. It slightly affects only the energy of intramolecular non-covalent interactions C(9)···O(carboxylate) due to the introduction of strong electron-withdrawing substituents. Both the carboxylate and nitro groups in these cases are practically coplanar to their benzene ring. Due to the orthogonal geometry, no conjugations between the π-systems of xanthene and phenyl moieties are expected.

The situation changes when a nitro group is introduced into positions 3′ or 6′. The first case is an example of classical steric repulsion between two bulky groups in *ortho*-positions in the same benzene ring. To minimize repulsion, both groups are rotated on a certain angle out of the ring plane (58° for the carboxylate and 40° for the nitro group). In this case, the C(9)···O(nitro) intramolecular interaction significantly weakens

and, apparently, has little effect on the dianion geometry. No bond path and corresponding (3, –1) critical point were further observed. Thus, it is impossible to estimate the energy of the C(9)···O(carboxylate) non-covalent intramolecular interaction for the 3′-nitro substituted fluorescein dianion. The angle between the planes of xanthene and side benzene rings decreases to 71°, which allows weak conjugation between the fragments under discussion to appear. This may be the reason for a certain long-wavelength shift in the absorption spectrum of 3′-nitrofluorescein dianion, which is also accompanied by an increase in molar absorptivity.

The nitro group in position 6′ also decreases the degree of mutual orthogonality of the main subunits of the dianion core, however, by a fundamentally different mechanism. Carboxylate and nitro groups are both attracted to the C(9) atom, but from different sides of the xanthene moiety. The discussed interaction is concurrent, and it is regulated by attraction forces between the partially negatively charged oxygen atoms of the nitro and carboxylate moieties and partially positive charged C(9) atom. The distance from C(9) to the nearest oxygen atom of the nitro group is about 2.77 Å, and the interaction energy calculated by the Espinosa approach [20] is ~3.29 kcal/mol. These parameters are quite close to those of the carboxylate group (Table 6). To equilibrate this "double-sided" concurrent interaction, the substituents move out of the plain of their common benzene ring: the carboxylate and nitro groups rotate by 20° and 41°, respectively. As a result, the angle between the xanthene and benzene fragments decreases to 72°, which requires the appearance of a certain (weak) conjugation between these fragments. This can lead to a slight bathochromic shift in the experimentally measured long-wavelength absorption band and an increase in the intensity of the latter.

In future, we plan to study the acid–base and tautomeric equilibria of compounds **2** and **5** in solution, thereby continuing the systematic study of the nitro- and amino derivatives of fluorescein [27,36]. The thermodynamic pK_a values for compounds **6** and **7** in DMSO at 25 °C, have already been determined as 10.46 ± 0.07 and 11.12 ± 0.07, respectively [39].

3. Experimental

3.1. Materials

DMSO was purified by freezing and distilling under vacuum; the water content was around 0.02% as determined by the coulometric Karl Fischer method. Acetonitrile stored for several days over P_4O_{10} and high-quality acetone were distilled over dehydrated K_2CO_3. The water content was around 0.01%. Diazabicyclo [5.4.0]undec-7-ene (DBU) was used as purchased from Merck.

3.2. Apparatus

Absorption spectra of the dyes were run on a Hitachi U-2000 spectrophotometer against the solvent blanks at 25 °C. Steady-state fluorescence spectra were obtained with a Perkin-Elmer FL6500 apparatus. The ^{1}H and ^{13}C NMR spectra were recorded on a Varian VNMRS-400 Spectrometer (^{1}H: 400 MHz; ^{13}C: 100 MHz). The NMR chemical shifts (δ) are reported in ppm downfield from tetramethylsilane as an internal reference. ESI mass spectra were obtained with a Waters Quattro Micro API Mass Spectrometer, and the solvent was methanol with 0.1% of formic acid. X-ray diffraction studies were performed at room temperature on an «Xcalibur-3» diffractometer (MoKα radiation, CCD-detector, graphite monochromator, ω-scanning, 2θmax = 52°).

3.3. Synthesis of the Dyes

In all syntheses, the final substances were preliminarily dried for 1 h at 100 °C and then for 2 h at 120 °C and 60 mmHg, unless otherwise noted.

3.3.1. Synthesis, Separation, and Purification of 3′-Nitrofluorescein and 6′-Nitrointermediate

A 21.11 g (0.100 mol) of 3-nitrophthalic acid was placed into a quartz test tube (H = 25 cm, D = 5 cm) and gently heated on a gas burner until the substance melted and the release of water vapor ceased. Then, the melt of anhydride of 3-nitrophthalic acid (18.90 g, 97.8%) was cooled and 16.00 g (0.1453 mol) of resorcinol was added. The mixture was heated in an oil bath at 190 ± 3 °C and stirred with a glass rod. After 30 min, the mixture thickened strongly due to precipitated small crystals. Then, 4.00 g (0.0363 mol) resorcinol was added. After 1 h, another 4.00 g (0.0363 mol) of resorcinol was added, and after 1.5 h the same amount of this compound was added again. Thus, the total amount of resorcinol was 28.00 g (0.2543 mol), and the total reaction time was 3 h. Then, the test tube was tilted and, rotating around the axis, the melt was evenly distributed over the walls of the vessel while cooling to 100 °C. Next, 60 mL of hot acetic acid was added to the test tube and the melt was dissolved with good mechanical stirring and heating. At this stage, the crystals stand out from the melt with the formation of a dark brown solution. The mixture was cooled, and the crystals were collected on a glass filter and washed thoroughly with 40 mL of acetic acid. The yield was 11.95 g of mustard-colored small crystals. The substance is a mixture of 6′-nitrointermediate and 3′-nitrofluorescein in the molar ratio 1:1, as follows from the NMR data. After 3 weeks, 6 g of the 6′-nitrointermediate was precipitated from the filtrate. The synthesis was carried out several times to accumulate the substance.

To 33.00 g of the dried substance obtained by the above method, 60 mL of dry acetone was added, and the mixture was stirred on a magnetic stirrer for 15 min at low boiling. A day later, the precipitate was collected and washed with 20 mL of acetone with the addition of 0.5 mL of acetic acid. The yield was 21.14 g. The product was retreated with 100 mL of hot acetone with an addition of 1 mL of acetic acid. The yield of crude 3′-nitrofluorescein was 19.85 g (17–20% with respect to the initial 3-nitrophthalic acid). The filtrates were combined and evaporated to dryness. The yield of crude 6′-nitrointermediate was 13.50 g; the admixture of 3′-nitrofluorescein was about 3%.

The diacetate of 3′-nitrofluorescein (4-nitro-3-oxo-3H-spiro[isobenzofuran-1,9′-xanthene]-3′,6′-diyl diacetate) 4. A mixture of 19.85 g crude 3′-nitrofluorescein with 40 mL of acetic anhydride and 0.40 mL of pyridine was refluxed for 2 h. Then 10 mL of the liquid were distilled off, and after adding 60 mL of hot acetic acid, the solution was cooled down to 25 °C, accompanied by stirring by a glass rod. The precipitated small crystals of 3′-nitrofluorescein diacetate were left at 6 °C for a day. They were then collected and washed with 10 mL of acetic acid (with the addition of 1 mL of acetic anhydride) and then with 10 mL of ethanol. The yield was 20.12 g of slightly yellow crystals with m.p. 221–222 °C. The substance was recrystallized from a mixture of 40 mL of acetic anhydride and 50 mL of acetic acid. The yield was 18.65 g (78.2%) of almost colorless crystals with m.p. 222 °C. ^{1}H NMR (400 MHz, DMSO-d_6), δ/ppm: 8.26 (1H, d, J = 7.8 Hz, **4′**), 8.02 (1H, t, J = 7.8 Hz, **5′**), 7.77 (1H, d, J = 7.8 Hz, **6′**), 7.31 (2H, d, J = 2.3 Hz, **4, 5**), 7.09 (2H, d, J = 8.8 Hz, **1, 8**), 6.97(2H, dd, J = 2.3 Hz, J = 8.8, Hz, **2, 7**), 2.29 (6H, s, **PhOCOC*H*$_3$**).

The crystals of 3′-nitrofluorescein diacetate for the X-ray analysis were prepared by recrystallization from acetic acid with 10% acetic anhydride.

X-ray diffraction study: Crystals of 3′-nitrofluorescein diacetate ($C_{24}H_{15}NO_9$, Mr = 461.37) are monoclinic, $P2_1/n$, a = 8.0908(3), b = 22.6112(14), c = 11.8909(5) Å, β = 108.086(5)°, V = 2067.87(18) Å^3, Z = 4, d_{calc} = 1.482 g cm^{-1}, μ = 0.116 mm^{-1}, F(000) = 952. A total of 7936 reflections (3630 independent, R_{int} = 0.078) were collected on an «Xcalibur-3» diffractometer (MoKα radiation, CCD-detector, graphite monochromator, ω-scanning, 2θ_{max} = 50°). The structure was solved by direct methods and refined against F^2 within anisotropic approximation for all non-hydrogen atoms by a full-matrix least squares procedure using the OLEX2 program package [40] with SHELXT [41] and SHELXL modules [42]. All H atoms were placed in idealized positions (C–H = 0.93–0.96 Å) and constrained

to ride on their parent atoms, with $U_{iso} = 1.2U_{eq}$ (except $U_{iso} = 1.5U_{eq}$ for methyl groups). The final refinement was converged at $wR_2 = 0.118$ for all 3630 reflections ($R_1 = 0.080$ for 2253 reflections with $F > 4\sigma(F)$, S = 1.025).

The atom coordinates and crystallographic parameters have been deposited with the Cambridge Crystallographic Data Centre (CCDC 2231735). These data can be obtained free of charge from the Cambridge Crystallographic Data Centre via www.ccdc.cam.ac.uk/data_request/cif, from 20/12/2022.

The triacetate of the 6′-nitrointermediate (4-(1-acetoxy-7-nitro-3-oxo-1,3-dihydroisobenzofuran-1-yl)-1,3-phenylene diacetate) 3. A mixture of 24.00 g of the crude 6′-nitrointermediate with 48 g acetic anhydride and 7.2 g pyridine was refluxed for 4 h. Then the solution was cooled, and after stirring with a glass rod, the crystals of the product separated out. The next day, the crystals were collected, washed with 10 mL of acetic acid and then with 5 mL of ethanol. The yield of the slightly yellow crystals was 25.75 g (75.8%). The substance was recrystallized from a mixture of 20 mL acetic anhydride with 20 mL of acetic acid. The yield of the colorless crystals was 24.90 g (73.3%) with m.p. 178 °C. ^{1}H NMR (400 MHz, DMSO-d_6), δ/ppm: 8.55 (1H, d, J = 8.0 Hz, **5′**), 8.49 (1H, d, J = 7.6 Hz, **3′**), 8.17 (1H, d, J = 8.8 Hz, **1**), 8.05 (1H, t, J = 7.9 Hz, **4′**), 7.26 (1H, dd, J = 2.1 Hz, J = 8.8 Hz, **2**), 7.03 (1H, d, J = 2.1 Hz, **4**), 2.27 (3H, s, **7** (**OCO*CH*$_3$**)), 2.23 (3H, s, **5** (**OCO*CH*$_3$**)), 1.70 (3H, s, **3** (**OCO*CH*$_3$**)).

The crystals of the 6′-nitrointermediate triacetate for the X-ray analysis were prepared by recrystallization from acetic anhydride.

X-ray diffraction study: Crystals of 6′-nitrointermediate triacetate ($C_{20}H_{15}NO_{10}$, Mr = 429.33) are triclinic, P $\bar{1}$, a = 8.7679(5), b = 10.0468(5), c = 11.6234(12) Å, α = 100.871(7)°, β = 93.767(7)°, γ = 104.772(4)°, V = 965.28(13) Å^3, Z = 2, d_{calc} = 1.477 g cm^{-1}, μ = 0.121 mm^{-1}, F(000) = 444. A total of 6200 reflections (3391 independent, R_{int} = 0.052) were collected on an «Xcalibur-3» diffractometer (MoKα radiation, CCD-detector, graphite monochromator, ω-scanning, $2\theta_{max}$ = 50°). The structure was solved by direct methods and refined against F^2 within anisotropic approximation for all non-hydrogen atoms by a full-matrix least squares procedure using the OLEX2 program package [40] with the SHELXT [41] and SHELXL modules [42]. All the H atoms were placed in idealized positions (C–H = 0.93–0.96 Å) and constrained to ride on their parent atoms, with $U_{iso} = 1.2U_{eq}$ (except $U_{iso} = 1.5U_{eq}$ for methyl groups). The final refinement was converged at $wR_2 = 0.081$ for all 3391 reflections ($R_1 = 0.069$ for 2797 reflections with $F > 4\sigma(F)$, S = 1.119).

The atom coordinates and crystallographic parameters have been deposited with the Cambridge Crystallographic Data Centre (CCDC 2231734). These data can be obtained free of charge from the Cambridge Crystallographic Data Centre via www.ccdc.cam.ac.uk/data_request/cif from 20/12/2022.

3′-Nitrofluorescein (3′,6′-dihydroxy-4-nitro-3H-spiro[isobenzofuran-1,9′-xanthen]-3-one) 2. A mixture of 7.00 g of 3′-nitrofluorescein diacetate, 70 mL of 10% aqueous NaOH solution, and 140 mL of methanol was heated for 20 min at 60 °C until a transparent solution formed. Then the solution was filtered, and the filtrate was diluted with water to 420 mL. The obtained solution was heated to 90 °C, and 35 mL of acetic acid was added. After a few seconds, a finely crystalline carrot-colored precipitate began to appear. The next day, the precipitate was collected and washed with 2% aqueous acetic acid. The yield was 5.65 g (98.7%); the substance in air gradually increased in mass to 5.92 g, which corresponds to 1 mol water per 1 mol of 3′-nitrofluorescein. ^{1}H NMR (400 MHz, DMSO-d_6), δ/ppm: 10.21 (2H, s, **Ph*OH***), 8.19 (1H, d, J = 7.7 Hz, **4′**), 7.98 (1H, t, J = 7.7 Hz, **5′**), 7.61 (1H, d, J = 7.7 Hz, **6′**), 6.72 (2H, d, J = 8.7 Hz, **1, 8**), 6.69 (2H, d, J = 2.1 Hz, **4, 5**), 6.57 (2H, dd, J = 2.1 Hz, J = 8.7 Hz, **2, 7**).

6′-Nitrointermediate (2-(2,4-dihydroxybenzoyl)-3-nitrobenzoic acid) 1:

(i) A mixture of 2.00 g 6′-nitrointermediate triacetate, 8 mL of acetic acid, and 1.0 mL of 70% aqueous methanesulfonic acid (MSA) was refluxed for 30 min. The solution was cooled, and the crystallization was initiated by stirring with a glass rod. The solution

was left overnight at 6 °C. The next day, small colorless crystals were collected on a glass filter, washed with 5 mL of acetic acid and three portions of water of 10 mL each. The precipitate became heavy with lemon-colored grains. The yield was 1.25 g (88.4%), with m.p. 258–260 °C. ^{1}H NMR (400 MHz, DMSO-d_6), δ/ppm: 13.28 (1H, brs, **2′** (**CO*OH***)), 11.56 (1H, brs, **5** (**Ph*OH***)), 10.58 (1H, brs, **3** (**Ph*OH***)), 8.42 (1H, d, *J* = 7.9 Hz, **5′**), 8.32 (1H, d, *J* = 7.7 Hz, **3′**), 7.85 (1H, brm, **4′**), 7.11 (1H, brs, **1**), 6.29 (2H, m, **2, 4**).

(ii) A mixture of 2.00 g 6′-nitrointermediate triacetate, 3 mL of acetic acid, and 1.0 mL of 70% aqueous MSA was refluxed for 15 min. Then 6.0 mL of hot water was added and the solution was slowly cooled. The next day, the lemon-colored crystals were collected and washed with water. The yield was 1.33 g (94.1%).

(iii) A 2.00 g of crude 6′-nitrointermediate was recrystallized from 12.5 mL of acetic acid. The yellow crystals were collected and washed with 4 mL of acetic acid. The yield was 1.44 g (72.0%), with m.p. 256 °C.

3.3.2. Synthesis of 3′-Aminofluorescein

3′-Aminofluorescein (4-amino-3′,6′-dihydroxy-3H-spiro[isobenzofuran-1,9′-xanthen]-3-one) 5. A mixture of 9.23 g (0.020 mol) of 3′-nitrofluorescein diacetate and 28.82 g (0.120 mol) $Na_2S \times 9H_2O$ in 150 mL of water was refluxed for 2 h. Then, the dark-brown solution was cooled, diluted with water to 300 mL, and 30 mL of acetic acid was added under stirring. The precipitate that formed was thoroughly stirred to a homogeneous consistency, collected and washed with two portions of 50 mL of 1% aqueous acetic acid. The yield was 7.03 g.

The crude 3′-aminofluorescein was dissolved in 40 mL of warm ethanol and the solution was filtered through a membrane filter. Then, a mixture of 64 mL of acetic acid with 15 mL of 35% HCl, preliminarily heated to 60 °C, was added to the clear filtrate. The solution was cooled to 6 °C. The next day, the precipitated burgundy-colored heavy crystals were collected on a glass filter and washed with two portions of acetic acid, 7 mL each. The yield was 7.30 g.

A 7.30 g of hydrochloric acid salt of 3′-aminofluorescein was dissolved in 100 mL of aqueous solution of NaOH (5.56 g). To the obtained solution, 0.10 g of activated charcoal was added. The solution was then heated to 60 °C, and after 10 min, it was cooled and filtered. The filtrate was diluted with water to 350 mL. Then, 17.0 g of acetic acid in 50 mL of water was added to the clear solution with constant stirring. The next day, the liquid was drained from the precipitate, water was added to 400 mL, thoroughly mixed on a magnetic stirrer, and again left for a day. The precipitate was collected on a glass filter and twice washed with 70 mL of water. The yield of light-yellow powder of 3′-aminofluorescein was 5.95 g (85.6%). ^{1}H NMR (400 MHz, DMSO-d_6), δ/ppm: 10.03 (2H, brs, **Ph*OH***), 7.35 (1H, t, *J* = 7.9 Hz, **5′**), 6.76 (1H, d, *J* = 8.3 Hz, **6′**), 6.66 (2H, d, *J* = 8.7 Hz, **1,8**), 6.65 (2H, d, *J* = 2.2 Hz, **4, 5**), 6.57 (2H, dd, *J* = 2.2 Hz, *J* = 8.7 Hz, **2, 7**), 6.47 (2H, brs, **Ph*NH*$_2$**), 6.18 (1H, d, *J* = 7.3 Hz, **4′**).

3.3.3. Synthesis of 3′-Nitrofluorescein and 3′-Aminofluorescein Methyl Esters

Methyl ester of 3′-nitrofluorescein (methyl 2-(6-hydroxy-3-oxo-3H-xanthen-9-yl)-6-nitrobenzoate) 6. A mixture of 0.395 g (0.001 mol) 3′-nitrofluorescein monohydrate, 0.400 mL of 99% sulfuric acid, and 10 mL of anhydrous methanol was boiled under reflux (with a desiccant tube attached to the top of condenser). After 40 h, the reaction mixture was cooled, diluted with 5 mL of methanol, and a solution of 0.70 g. NaOH in 100 mL of water was added with constant stirring in small portions up to pH 12. Then, a 10% aqueous KH_2PO_4 solution was added dropwise to pH 11, and after adding activated charcoal, the solution was filtered through a fine-pore glass filter. The filtrate was diluted with water to 125 mL and acidified with the above mentioned KH_2PO_4 solution to pH 7.0. A very fine red precipitate of the 3′-nitrofluorescein methyl ester appeared. The next day, the precipitate was collected on a fine-pore glass filter and washed with a mixture of 30

mL of water and 3 mL of methanol. The yield of the red powder was 0.30 g (77%). ^{1}H NMR (400 MHz, DMSO-d_6), δ/ppm: 11.21 (1H, brs, **Ph*OH***), 8.44 (1H, d, *J* = 8.1 Hz, **4′**), 8.02 (1H, t, *J* = 8.1 Hz, **5′**), 7.96 (1H, d, *J* = 8.1 Hz, **6′**), 6.86 (2H, d, *J* = 9.3 Hz, **1, 8**), 6.59 (4H, brm, **2, 7, 4, 5**), 3.45 (3H, s, **PhCOO*CH*$_3$**).

Methyl ester of 3′-aminofluorescein (**methyl 2-amino-6-(6-hydroxy-3-oxo-3H-xanthen-9-yl)benzoate) 7**. A mixture of 0.347 g (0.001 mol) 3′-aminofluorescein, 0.500 mL of 99% sulfuric acid, and 10 mL of anhydrous methanol was boiled under reflux (with a desiccant tube attached to the top of the condenser). After 60 h, the reaction mixture was cooled, filtered, and made up with methanol to 12 mL. Then, 0.645 g imidazole was added under stirring with a glass rod. Brown crystals of 3′-aminofluorescein methyl ester began to precipitate almost immediately. A day later, the crystals were collected on a glass filter and washed with 2 mL of acetone. The yield was 0.24 g (66%). ^{1}H NMR (400 MHz, DMSO-d_6), δ/ppm: 7.38 (1H, dd, *J* = 8.3 Hz, *J* = 7.3 Hz, **5′**), 7.01 (1H, d, *J* = 8.3 Hz, **6′**), 6.97 (2H, d, *J* = 9.3 Hz, **1, 8**), 6.70–6.47 (6H, brm, **2, 7, 4, 5, Ph*NH*$_2$**), 6.44 (1H, d, *J* = 7.3 Hz, **4′**), 3.30 (3H, s, **PhCOO*CH*$_3$**).

Syntheses of methyl esters of 3′-nitrofluorescein and 3′-aminofluorescein can be carried out in hermetically sealed thick-walled glass test tubes at 95–100 °C in compliance with safety measures. In this case, the reaction time is reduced by 10 times. However, in addition to the main product, the content of impurities also increases, the main of which is dimethyl ester–ether of 3′-nitro (3′-amino) fluorescein, according to the NMR data.

3.3.4. Some Additional Experiments

As mentioned above, when 3-nitrophthalic anhydride is fused with resorcinol, only 3′-nitrofluorescein **2** and 6′-nitrointermediate **1** are formed. The 6′-nitrofluorescein **M2** is formed under these conditions in very small amounts, as follows from the NMR spectra of the melt. In order to obtain 6′-nitrofluorescein **M2**, we carried out a number of trial syntheses based on the 6′-nitrointermediate **1**. Thus, when 0.10 g of the 6′-nitrointermediate **1**, 0.10 g of resorcinol, and 0.50 g of *p*-toluenesulfonic acid were fused at 130 °C for 1 h, a dark-colored melt was obtained, which was treated with hot water upon cooling. The oil that appeared on the walls of the vessel was separated by decantation, then dissolved in 1% NaOH, and the resulting solution was neutralized with 10% HCl. The precipitate was collected, washed with water and dried. The yield of crude 6′-nitrofluorescein **M2** was about 1.5 mg. The ^{1}H NMR spectrum is given in the Supplementary Material. ^{1}H NMR (400 MHz, DMSO-d_6), δ/ppm: 10.12 (2H, s, Ph*OH*), 8.61 (1H, d, *J* = 7.9 Hz, **5′**), 8.49 (1H, d, *J* = 7.9 Hz, **3′**), 8.07 (1H, t, *J* = 7.9 Hz, **4′**), 6.67 (2H, d, *J* = 2.4 Hz, **4, 5**), 6.64 (2H, d, *J* = 8.8 Hz, **1, 8**), 6.47 (2H, dd, *J* = 2.4 Hz, *J* = 8.8 Hz, **2, 7**).

When trying to obtain a 3′-nitrointermediate **M1** by saponification of 3′-nitrofluorescein **2** in concentrated alkali, it turned out unexpectedly that the reaction produces 3′-aminofluorescein **5**. A 0.20 g of 3′-nitrofluorescein **2** was dissolved in 10 g of 20% NaOH, and the resulting solution was refluxed for 30 min. The reaction course was monitored by measuring the electronic absorption spectra: the initial absorption band with a maximum at 501 nm completely disappeared and an absorption band with a maximum at 490 nm appeared.

The dark brown reaction mixture was cooled, neutralized with 5 mL of 33% HCl to pH 6–7, diluted with 5 mL water and stirred for 15 min on a magnetic stirrer. The precipitate was collected, washed with water and dried. A yield 0.12 g of the crude product was obtained, in which the content of 3′-aminofluorescein **5** was 70.7%. The ^{1}H and ^{1}H-^{1}H COSY NMR spectra are given in the Supplementary Material.

Next, 30 mL of the filtrate was dried at 100–105 °C. The residue was then treated with several portions of acetone (10 mL), and the extract was filtered through a membrane filter and dried. A Yield 0.030 g of crude 3′-nitrointermediate **M1** was obtained. Monoisotopic mass: 303.04. ESI MS: 303.96 [M + H]+, 301.77 [M − H]−. The ^{1}H and ^{1}H-^{1}H COSY NMR spectra are given in the Supplementary Material. ^{1}H NMR (400 MHz, DMSO-d_6), δ/ppm: 13.67 (1H, brs, CO*OH*), 11.79 (1H, brs, Ph*OH*), 10.95 (1H, brs, Ph*OH*),

8.14 (1H, d, *J* = 6.2 Hz, **4′**), 7.83–7.74 (2H, d, t, *J* = 6.2 Hz, **5′**, **6′**), 7.18 (1H, d, *J* = 8.7 Hz, **1**), 6.36 (1H, dd, *J* = 8.7 Hz, *J* = 2.2 Hz, **2**), 6.33 (1H, d, *J* = 2.2 Hz, **4**).

Upon saponification of 3′-nitrofluorescein **2** under harsher conditions, the resulting 3′-aminofluorescein decomposes into a number of unidentified products, the main of which is the 3′-aminointermediate **M3**. Monoisotopic mass: 273.06. ESI MS: 273.86 [M + H]+, 271.83 [M − H]−. The ^{1}H, ^{13}C and ^{1}H-^{1}H COSY NMR spectra are given in the Supplementary Material.

(i) A mixture of 0.20 g of 3′-nitrofluorescein and 4.0 g of 50% NaOH was heated at 85–90 °C for 5 h. The reaction course was monitored by measuring the electronic absorption spectra. The solution was then cooled, acidified with 10% HCl to pH 6–7 and filtered. The filtrate was dried at 100–105 °C. The residue was then treated with several portions of acetone (10 mL), and the extract was filtered through a membrane filter and dried. The yield was 0.060 g of dry residue.

(ii) A mixture of 0.20 g of 3′-aminofluorescein and 4.0 g of 50% NaOH was heated at 100–105 °C for 2 h. Next, the product mixture was isolated as described above. A yield of 0.10 g of dry residue was obtained. The NMR spectrum was identical to case (i). To isolate the 3′-aminointermediate **M3**, the resulting mixture was dissolved in 0.5 mL of acetic acid, filtered and acidified with two drops of 35% HCl. The yellow precipitate was collected, washed with several portions of acetic acid and dissolved on heating in 0.5 mL of 50% aqueous ethanol. To the obtained hot solution, three drops of 35% HCl were added. On cooling, yellow crystals precipitated. The product was collected, washed with several portions of acetonitrile and dried. The yield was 0.030 g of 3′-aminointermediate **M3**. Monoisotopic mass: 273.06. ESI MS: 274.35 [M + H]+, 272.28 [M − H]−. ^{1}H NMR (400 MHz, DMSO-d_6), δ/ppm: 12.34 (1H, brs, Ph*OH*), 10.64 (1H, brs, Ph*OH*), 7.28 (1H, t, *J* = 7.8 Hz, **5′**), 7.04 (1H, d, *J* = 8.4 Hz, **1**), 6.90 (1H, d, *J* = 7.8 Hz, **6′**), 6.40 (1H, d, *J* = 7.8 Hz, **4′**), 6.29 (1H, d, *J* = 2.1 Hz, **4**), 6.28 (1H, dd, *J* = 8.4 Hz, *J* = 2.1 Hz, **2**).

4. Conclusions

Two dyes of the fluorescein series, 3′-nitrofluorescein and 3′-aminofluorescein, as well as their methyl esters, were synthesized and characterized by ^{1}H, ^{13}C NMR, and UV-visible spectroscopy, fluorescence spectra, and in some cases X-ray diffraction analysis. Some intermediates and by-products were isolated and identified.

The absorption spectra of double-charged anions, R^{2-}, of mononitro fluoresceins bearing the NO_2 group in different positions in the phthalic acid residue were considered. The influence of the 3′- and 6′-substitution on the position of absorption maximum is more pronounced than that of the 4′- and 5′-derivatives. This is in line with substitution-induced changes in the geometry of fluorescein, as investigated using a quantum-chemical method.

While the light emission of the R^{2-} 3′-nitrofluorescein dianion in solutions of various natures is very weak, the corresponding form of 3′-aminofluorescein exhibits beautiful bright fluorescence in DMSO, acetonitrile, and acetone, i.e., in solvents that are not hydrogen bond donors. However, even small additions of water lead to fluorescence quenching. This is consistent with the properties of nitro and amino derivatives of fluorescein-bearing substituents in 4′- and 5′-positions that were studied previously.

At present, 3′-aminofluorescein, synthesized here for the first time, can be used either as a fluorescent indicator sensitive to H-bonds or as a platform for reagents capable of covalent attachment to biomolecules, by analog with the well-studied 4′- and 5′-aminofluoresceins. In addition, it is planned to study the acid–base and tautomeric equilibria of compounds **2** and **5** in solution, thereby continuing the systematic study of the protolytic properties of fluorescein nitro- and amino derivatives.

Supplementary Materials: The following supporting information can be downloaded at: https://www.mdpi.com/article/10.3390/colorants2030024/s1, **Figure S1.** ^{1}H and ^{13}C NMR spectra of

3′-nitrofluorescein diacetate. **Figure S2.** ^{1}H and ^{13}C NMR spectra of 6′-nitrointermediate triacetate. **Figure S3.** ^{1}H and ^{13}C NMR spectra of 3′-nitrofluorescein. **Figure S4.** ^{1}H and ^{13}C NMR spectra of 6′-nitrointermediate. **Figure S5.** ^{1}H and ^{13}C NMR spectra of 3′-aminofluorescein. **Figure S6.** ^{1}H and ^{13}C NMR spectra of 3′-nitrofluorescein methyl ester. **Figure S7.** ^{1}H and ^{13}C NMR spectra of 3′-aminofluorescein methyl ester. **Figure S8.** ^{1}H NMR spectrum of 6′-nitrofluorescein, crude. **Figure S9.** ^{1}H and ^{1}H-^{1}H COSY NMR spectra of 3′-aminofluorescein, crude (obtained by heating of 3′-nitrofluorescein in concentrated alkali). **Figure S10.** ^{1}H and ^{1}H-^{1}H NMR spectra of 3′-nitrointermediate, crude. **Figure S11.** ^{1}H and ^{1}H-^{1}H NMR spectra of the mixture, obtained by decomposition of 3′-aminofluorescein in concentrated alkali with more intense heating. The main product of the reaction is assumed to be 3′-aminointermediate. **Figure S12.** ^{1}H and ^{13}C NMR spectra of 3′-aminointermediate.

Author Contributions: S.V.S. (Sergey V. Shekhovtsov): Conceptualization, Methodology, Validation, Investigation, Visualization, Resources, Writing—Original Draft. I.V.O.: Methodology, Software, Formal analysis, Visualization. S.V.S. (Svitlana V. Shishkina): Methodology, Software, Formal analysis, Resources, Writing—Original Draft. A.O.D.: Methodology, Software, Visualization, Writing—Original Draft, Writing—Review & Editing. K.O.V.: Investigation, Data curation. H.S.V.: Investigation, Data curation. N.O.M.-P.: Conceptualization, Supervision, Writing—review & editing, Project administration, Funding acquisition. All authors have read and agreed to the published version of the manuscript.

Funding: This study was partially supported by the Ministry of Education and Science of Ukraine via grant number 0122U001485.

Institutional Review Board Statement: Not applicable

Informed Consent Statement: Not applicable

Data Availability Statement: Structure **3** The atom coordinates and crystallographic parameters have been deposited with the Cambridge Crystallographic Data Centre (CCDC 2231734). These data can be obtained free of charge from the Cambridge Crystallographic Data Centre via www.ccdc.cam.ac.uk/data_request/cif. Structure **4** The atom coordinates and crystallographic parameters have been deposited with the Cambridge Crystallographic Data Centre (CCDC 2231735). These data can be obtained free of charge from the Cambridge Crystallographic Data Centre via www.ccdc.cam.ac.uk/data_request/cif.

Conflicts of Interest: The authors declare no conflict of interest.

References

1. Coons, A.H.; Kaplan, M.H. Localization of antigen in tissue cells: II. Improvements in a method for the detection of antigen by means of fluorescent antibody. *J. Exp. Med.* **1950**, *91*, 1–13. https://doi.org/10.1084/JEM.91.1.1.
2. Sigmund, H.; Pfleiderer, W. Nucleotides. Part LXXI: A new type of labelling of nucleosides and nucleotides. *Helv. Chim. Acta* **2003**, *86*, 2299–2334. https://doi.org/10.1002/HLCA.200390186.
3. Kuroiwa, T. Photodynamic diagnosis and photodynamic therapy for the brain tumors. *Prog. Neuro-Oncol.* **2014**, *21*, 4–21. https://doi.org/10.11452/neurooncology.21.3_14.
4. Bharate, G.Y.; Qin, H.; Fang, J. Poly(styrene-co-maleic acid)-conjugated 6-aminofluorescein and rhodamine micelle as macromolecular fluorescent probes for micro-tumors detection and imaging. *J. Pers. Med.* **2022**, *12*, 1650. https://doi.org/10.3390/jpm12101650.
5. Hongrapipat, J.; Kopecková, P.; Liu, J.; Prakongpan, S.; Kopecek, J. Combination chemotherapy and photodynamic therapy with fab' fragment targeted HPMA copolymer conjugates, in human ovarian carcinoma cells. *Mol. Pharm.* **2008**, *5*, 696–709. https://doi.org/10.1021/mp800006e.
6. Glushko, V.N.; Blokhina, L.I.; Sadovskaya, N.Y. Studies on the synthesis of fluorescein-5-isothiocyanate: A fluorescent nanomarker for biosensors. *Russ. J. Gen. Chem.* **2015**, *85*, 2458–2464. https://doi.org/10.1134/S1070363215100412.
7. Reverdin, F. Ueber einen gelben Farbstoff, welcher vom Dinitrofluoresceïn abstammt. *Berichte* **1897**, *30*, 332–334. https://doi.org/10.1002/cber.18970300166.
8. Bogert, M.T.; Wright, R.G. Some experiments on the nitro derivatives of fluorescein. *J. Am. Chem. Soc.* **1905**, *27*, 1310–1316. https://doi.org/10.1021/ja01988a015.
9. Moir, J. Colour and chemical constitution, Part II.—The spectra of the mixed phthaleins and of the sulphone-phthaleins. *Trans. R. Soc. S. Afr.* **1918**, *7*, 111–116. https://doi.org/10.1080/00359191809519549.
10. Moir, J. Colour and chemical constitution. Part XV. A systematic study of fluorescein and resorcin-benzein. *Trans. R. Soc. S. Afr.* **1922**, *10*, 159–164. https://doi.org/10.1080/00359192209519277.
11. Underwood, H.W.; Wakeman, R.L. Studies in the 3-nitrophthalic acid series. *J. Am. Chem. Soc.* **1931**, *53*, 1839–1842.

12. Hanna, C.; Smith, W.T. The absorption spectra of derivatives of phthalic anhydride. *Proc. Iowa Acad. Sci*. **1951**, *58*, 251–260.
13. Klonis, N.; Sawyer, W.H. Spectral properties of the prototropic forms of fluorescein in aqueous solution. *J. Fluoresc.* **1996**, *6*, 147–157. https://doi.org/10.1007/BF00732054.
14. DeRose, P.C.; Kramer, G.W. Bias in the absorption coefficient determination of a fluorescent dye, standard reference material 1932 fluorescein solution. *J. Lumin.* **2005**, *113*, 314–320. https://doi.org/10.1016/j.jlumin.2004.11.002.
15. Becke, A.D. Density-functional thermochemistry. III. The role of exact exchange. *J. Chem. Phys.* **1993**, *98*, 5648–5652. https://doi.org/10.1063/1.464913.
16. Dunning, T.H. Gaussian basis sets for use in correlated molecular calculations. I. The atoms boron through neon and hydrogen. *J. Chem. Phys.* **1989**, *90*, 1007–1023. https://doi.org/10.1063/1.456153.
17. Ruud, K.; Helgaker, T.; Bak, K.L.; Jørgensen, P.; Jensen, H.J.A. Hartree-Fock Limit Magnetizabilities from London Orbitals. *J. Chem. Phys.* **1993**, *99*, 3847–3859. https://doi.org/10.1063/1.466131.
18. Tomasi, J.; Mennucci, B.; Cammi, R. Quantum mechanical continuum solvation models. *Chem. Rev*. **2005**, *105*, 2999–3093. https://doi.org/10.1021/cr9904009.
19. Frisch, M.J.; Trucks, G.W.; Schlegel, H.B.; Scuseria, G.E.; Robb, M.A.; Cheeseman, J.R.; Scalmani, G.; Barone, V.; Mennucci, B.; Petersson, G.A.; et al. *Gaussian 09, Revision B.01*; Gaussian, Inc.: Wallingford, CT, USA, 2010.
20. Espinosa, E.; Molins, E.; Lecomte, C. Hydrogen bond strengths revealed by topological analyses of experimentally observed electron densities. *Chem. Phys. Lett.* **1998**, *285*, 170–173. https://doi.org/10.1016/S0009-2614(98)00036-0.
21. Bader, R.F.W. Atoms in molecules. *Acc. Chem. Res.* **1985**, *18*, 15–18. https://doi.org/10.1021/ar00109a003.
22. Bader, R.F.W. A quantum theory of molecular structure and its applications. *Chem. Rev*. **1991**, *91*, 893–928. https://doi.org/10.1021/cr00005a013.
23. Burgi, H.-B.; Dunitz, J.D. *Structure Correlation*; VCH: Weinheim, Germany, 1994; Volume 2, pp. 741–784.
24. Polyakova, I.N.; Starikova, Z.A.; Parusnikov, B.V.; Krasavin, I.A.; Dobryakova, G.M.; Zhadanov, B.V. The lactone form of fluorescein: Crystal structure of the 1:1 molecular complex of fluorescein with methanol. *J. Struct. Chem.* **1984**, *25*, 752–757. https://doi.org/10.1007/BF00747920.
25. Osborn, R.S.; Rogers, D. The crystal and molecular structure of the 1:1 complex of acetone with the lactoid form of fluorescein. *Acta Crystallogr. Sect. B Struct. Crystallogr. Cryst. Chem.* **1975**, *B31*, 359–364. https://doi.org/10.1107/S0567740875002804.
26. Arhangelskis, M.; Eddleston, M.D.; Reid, D.G.; Day, G.M.; Bucar, D.-K.; Morris, A.J.; Jones, W. Rationalization of the color properties of fluorescein in the solid state: A combined computational and experimental study. *Chem.-Eur. J.* **2016**, *22*, 10065–10073. https://doi.org/10.1002/chem.201601340.
27. Mchedlov-Petrossyan, N.O.; Cheipesh, T.A.; Shekhovtsov, S.V.; Ushakova, E.V.; Roshal, A.D.; Omelchenko, I.V. Aminofluoresceins vs fluorescein: Ascertained new unusual features of tautomerism and dissociation of hydroxyxanthene dyes in solution. *J. Phys. Chem. A* **2019**, *123*, 8845–8859. https://doi.org/10.1021/acs.jpca.9b05810.
28. Mchedlov-Petrossyan, N.O.; Cheipesh, T.A.; Shekhovtsov, S.V.; Redko, A.N.; Rybachenko, V.I.; Omelchenko, I.V.; Shishkin, O.V. Ionization and tautomerism of methyl fluorescein and related dyes. *Spectrochim. Acta A* **2015**, *150*, 151–161. https://doi.org/10.1016/j.saa.2015.05.037.
29. Suresh Kumar, G.S.; Seethalakshmi, P.G.; Bhuvanesh, N.; Kumaresan, S. Studies on the syntheses, structural characterization, antimicrobial-, and DPPH radical scavenging activity of the cocrystals caffeine:cinnamic acid and caffeine:eosin dihydrate. *J. Mol. Struct.* **2013**, *1050*, 88–96. https://doi.org/10.1016/j.molstruc.2013.07.018.
30. Hou, F.; Cheng, J.; Xi, P.; Chen, F.; Huang, L.; Xie, G.; Shi, Y.; Liu, H.; Bai, D.; Zeng, Z. Recognition of copper and hydrogen sulfide in vitro using a fluorescein derivative indicator. *Dalton Trans*. **2012**, *41*, 5799–5804. https://doi.org/10.1039/C2DT12462A.
31. He, H.; He, T.; Zhang, Z.; Xu, X.; Yang, H.; Qian, X.; Yang, Y. Ring-restricted *N*-nitrosated rhodamine as a green-light triggered, orange-emission calibrated and fast-releasing nitric oxide donor. *Chin. Chem. Lett.* **2018**, *29*, 1497–1499. https://doi.org/10.1016/j.cclet.2018.08.019.
32. Mchedlov-Petrossyan, N.O.; Cheipesh, T.A.; Roshal, A.D.; Shekhovtsov, S.V.; Moskaeva, E.G.; Omelchenko, I.V. Aminofluoresceins vs fluorescein: Peculiarity of fluorescence. *J. Phys. Chem. A* **2019**, *123*, 8860–8870. https://doi.org/10.1021/acs.jpca.9b05812.
33. Mchedlov-Petrossyan, N.O.; Cheipesh, T.A.; Roshal, A.D.; Doroshenko, A.O.; Vodolazkaya, N.A. Fluorescence of aminofluoresceins as an indicative process allowing to distinguish between micelles of cationic surfactants and micelle-like aggregates. *Methods Appl. Fluor*. **2016**, *4*, 034002. https://doi.org/10.1088/2050-6120/4/3/034002.
34. Poronik, Y.M.; Sadowski, B.; Szychta, K.; Quina, F.H.; Vullev, V.I.; Gryko, D.T. Revisiting the non-fluorescence of nitroaromatics: Presumption versus reality. *J. Mater. Chem. C* **2022,** *10*, 2870–2904. https://doi.org/10.1039/D1TC05423F.
35. Thomas, A.; Kirilova, E.M.; Nagesh, B.V.; Krishna Chaitanya, G.; Philip, R.; Manohara, S.R.; Sudeeksha, H.C.; Siddlingeshwar, B. Influence of nitro group on solvatochromism, nonlinear optical properties of 3-morpholinobenzanthrone: Experimental and theoretical study. *J. Photochem. Photobiol. A Chem.* **2023**, *437*, 114434. https://doi.org/10.1016/j.jphotochem.2022.114434.
36. Mchedlov-Petrossyan, N.O.; Cheipesh, T.A.; Moskaeva, E.G.; Shekhovtsov, S.V.; Ostrovskyi, K.I. Towards understanding of stepwise acid-base dissociation in systems inclined to tautomerism: Nitro derivatives of fluorescein in dimethyl sulfoxide. *J. Mol. Liquids* **2023**, *386*, 122540. https://doi.org/10.1016/j.molliq.2023.122540.
37. Zhao, Y.; Truhlar, D.G. The M06 suite of density functionals for main group thermochemistry, thermochemical kinetics, noncovalent interactions, excited states, and transition elements: Two new functionals and systematic testing of four M06-class functionals and 12 other functionals. *Theor. Chem. Acc.* **2008**, *120*, 215–241. https://doi.org/10.1007/s00214-007-0310-x.

38. Zhikol, O.A.; Shishkin, O.V. Estimating stacking interaction energy using atom in molecules properties: Homodimers of benzene and pyridine. *Int. J. Quant. Chem*. **2012**, *112*, 3008–3017. https://doi.org/10.1002/qua.24189.
39. Moskaeva, E.G.; Ostrovskiy, K.I.; Shekhovtsov, S.V.; Mchedlov-Petrossyan, N.O. Transmittance of electronic effects in the fluorescein molecule: Nitro and amino groups in the phthalic acid residue. *Kharkiv Univ. Bull*. **2021**, *36*, 24–32. https://doi.org/10.26565/2220-637X-2021-36-05.
40. Dolomanov, O.; Bourhis, L.; Gildea, R.; Howard, J.A.K.; Puschmann, H. OLEX2: A complete structure solution, refinement and analysis program. *J. Appl. Cryst.* **2009**, *42*, 339–341. https://doi.org/10.1107/S0021889808042726.
41. Sheldrick, G.M. SHELXT—Integrated space-group and crystal-structure determination. *Acta Crystallogr. Sect. A Found. Adv.* **2015**, *71*, 3–8. https://doi.org/10.1107/S2053273314026370.
42. Sheldrick, G.M. Crystal structure refinement with SHELXL. *Acta Crystallogr. Sect. C* **2015**, *71*, 3–8. https://doi.org/10.1107/S2053229614024218.